

Mössbauer study of FeCoSiAlGaPCB amorphous alloys

J. M. Borrego, C. F. Conde, and A. Conde^{a)}

Departamento de Física de la Materia Condensada, Instituto de Ciencia de Materiales, C.S.I.C., Universidad de Sevilla, P.O. Box 1065, 41080 Sevilla, Spain

S. Roth and J. Eckert^{b)}

Leibniz Institut für Metallische Werkstoffe, IFW Dresden, Postfach 270016, D-01171 Dresden, Germany

J. M. Greneche

Laboratoire de Physique de l'Etat Condensé, UMR CNRS 6087, Université du Maine, F-72085 Le Mans Cedex 9, France

(Received 10 November 2003; accepted 21 January 2004)

A Mössbauer spectrometry and magnetic study have been performed on FeCoSiAlGaPCB amorphous alloys in order to get information about the variations in the atomic short range order with the substitution of Fe by Co. The decrease of the Curie temperature with decreasing Fe content was analyzed in the framework of the molecular field theory. The average hyperfine magnetic field at 77 K decreases linearly with increasing Co content as does the average magnetic moment per transition metal atom and a linear dependence between both quantities is found. The standard deviation of the hyperfine magnetic field distribution at 77 K does not change with Fe substitution and the average isomer shift increases linearly with the Co content of the alloy. The hyperfine magnetic field distributions show a bimodal character that evidences the presence of two types of Fe environments in the as-cast alloys. © 2004 American Institute of Physics.

[DOI: 10.1063/1.1682689]

I. INTRODUCTION

The development of multicomponent amorphous soft magnetic materials with low critical cooling rate for glass formation and a wide supercooled liquid region before crystallization has become an important research topic in recent years.¹ Amorphous FeSiAlGaPCB are known to have interesting soft magnetic properties combined with good glass-forming ability, promising technological applications of bulk soft magnetic materials. The replacement of Fe by Co is known to affect the glass forming ability and the magnetic properties of these alloys.²

Chemical and topological short range order changes in transition metal-metalloid alloys can be studied by macroscopic magnetization measurements and additionally by microscopic experimental methods, among which those based on hyperfine interactions (nuclear magnetic resonance and Mössbauer spectrometry) are believed to provide relevant information that reflects the variety of local surroundings of resonant absorbing nuclei.

In the present work Mössbauer spectrometry and magnetic measurements have been used to study multicomponent Fe_yCo_zB_uC_wSi₃Al₅Ga₂P₁₀ amorphous alloys (Table I) in order to get information about the effect of substitution of the transition metal atom in these metal-metalloid amorphous alloys.

Mössbauer spectrometry is an especially useful tool for studying amorphous alloys, where a variety of environments must exist for each atomic species. It serves as a sensitive probe of the average values of properties like the isomer shift (IS) and the hyperfine magnetic field (B_{hf}). Even more important, it brings out the distribution of the hyperfine magnetic field which may show whether iron nuclei are sensing the more or less uniform distribution of local fields or whether there are two or more nonequivalent positions of iron in the alloy. The average values of IS and B_{hf} distributions often exhibit easily measurable composition dependences which can be used to study some connections between the amorphous structure and the measured data.

II. EXPERIMENT

Multicomponent Fe_yCo_zB_uC_wSi₃Al₅Ga₂P₁₀ alloys (Table I) were prepared by arc melting under argon atmosphere. Raw materials of high purity were used; metals: 99.99%, FeC and FeB: 99.5%, FeP: 97.5%. From these alloys, 10 mm wide and 25- μm -thick amorphous ribbons were prepared by single-roller melt spinning.

The Curie temperature, T_C , was determined from magnetization versus temperature, $M(T)$, curves measured with a Faraday magnetometer in a field of 460 kA m⁻¹, fitting the data below T_C to a critical law of the form $M(T) \propto (T - T_C)^\beta$ with $\beta=0.36$ and extrapolating to $M=0$. Mössbauer spectra were taken at 77 and 300 K in a transmission geometry using a ⁵⁷Co(Rh) source, with the γ -beam perpendicular to the ribbon plane. The values of hyperfine parameters were refined using NORMOS program.³ The isomer shift values are quoted relative to α -Fe at 300 K.

^{a)}Electronic mail: conde@us.es

^{b)}Present address: TUDarmstadt, FB11 Material-und Geowissenschaften, FG Physikalische Metallkunde, Petersenstrasse 23, D-64287 Darmstadt, Germany

TABLE I. Composition of $\text{Fe}_y\text{Co}_z\text{B}_u\text{C}_w\text{Si}_3\text{Al}_5\text{Ga}_2\text{P}_{10}$ amorphous alloys.

Alloy	A	B	C	D	E	F
y	70	56	43	29	17	5
z	0	14	26	40	52	63
u	5	6	8	9	10	12
w	5	4	3	2	1	0
$x = z/(y+z)$	0	0.2	0.4	0.6	0.75	0.9

III. RESULTS AND DISCUSSION

A. Curie temperature

The Curie temperature of the alloys, shown in Fig. 1 as a function of their relative Co/(Fe+Co) concentration, x , decreases monotonously as the Co content of the alloy increases. This dependence of T_C is similar to that found in $(\text{Fe}_{1-x}\text{Co}_x)_{62.5}\text{Si}_{12.5}\text{B}_{25}$ alloys,⁴ but different to that observed in amorphous Fe–Co based alloys with lower metalloid content, for which T_C shows a maximum for equiatomic Fe/Co compositions.^{5,6} Curie temperature values were analyzed following a phenomenological model based on the molecular field theory,⁷ that accounts for the dependence of T_C of an amorphous ferromagnetic alloy with two different moments on it, as a function of their relative concentration, x . If the variation of the magnitude of the individual atomic moments with composition is assumed to be small, the equation describing $T_C(x)$ can be expressed as

$$T_C(x) = \frac{1}{2}[T_{\text{FeFe}}(1-x) + T_{\text{CoCo}x}] + \left\{ \frac{1}{4}[T_{\text{FeFe}}(1-x) - T_{\text{CoCo}x}]^2 + T_{\text{FeCo}}^2 x(1-x) \right\}^{1/2}, \quad (1)$$

where T_{FeFe} , T_{CoCo} , and T_{FeCo} are related to the exchange interactions of Fe–Fe, Co–Co, and Fe–Co pairs, respectively. The overall behavior of our $T_C(x)$ data is well described using Eq. (1) as can be observed in Fig. 1 (solid line). Best fitting values for T_{FeFe} , T_{CoCo} , and T_{FeCo} are 575, 269, and 525 K, respectively. Therefore, the strong decrease of T_C with increasing Co content can be ascribed to the lower value of the Co–Co exchange interaction compared to that of Fe–Fe.

However, an analogous analysis on Curie temperature values of amorphous Co-containing FINEMET-type alloys with composition $(\text{Fe}_{1-x}\text{Co}_x)_{73.5}\text{Si}_{13.5}\text{B}_9\text{Nb}_3\text{Cu}_1$ ⁸ gives $T_{\text{FeFe}} = 590$ K, $T_{\text{CoCo}} = 656$ K, and $T_{\text{FeCo}} = 725$ K. A stronger

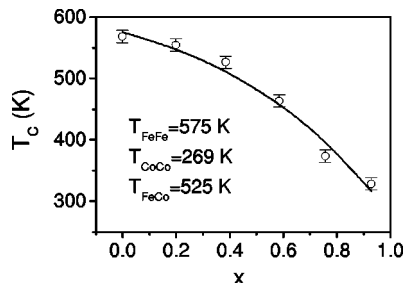


FIG. 1. Curie temperature, T_C , of $\text{Fe}_y\text{Co}_z\text{B}_u\text{C}_w\text{Si}_3\text{Al}_5\text{Ga}_2\text{P}_{10}$ (Table I) amorphous alloys as a function of their relative Co/(Fe+Co) content, x . Solid line: the simulation curve according to Eq. (1). T_{FeFe} , T_{CoCo} , and T_{FeCo} are the parameters that best fit the experimental data.

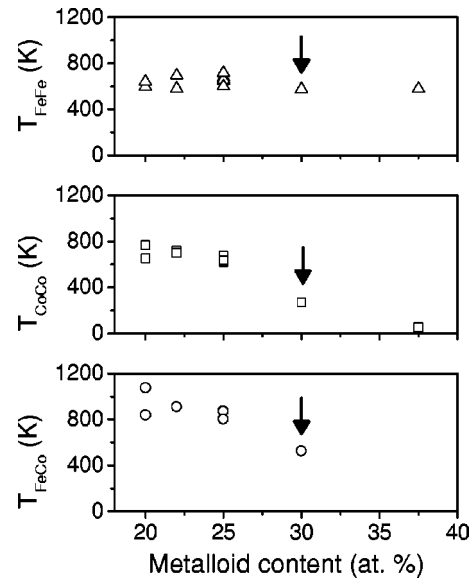


FIG. 2. Compilation of T_{FeFe} , T_{CoCo} , and T_{FeCo} for some Fe–Co based amorphous alloys as a function of their metalloid content. (see Refs. 4–6, 9) The arrows point to the values corresponding to the alloys of the present study.

exchange interaction between Co–Co atoms pairs compared to that of Fe–Fe atoms pairs could explain the increase in T_C with Co content in these alloys series. Figure 2 shows the interaction temperatures for several Fe–Co based amorphous alloys as a function of their metalloid (B,Si,P,Al,C) content, varying from 20 to 37.5 at. %.^{4–6,9} The arrows point to the values corresponding to the alloys object of the present study. For alloys with metalloid content $\geq 30\%$, the Fe–Fe exchange interaction temperature is significantly stronger than that of Co–Co atoms pairs, while only slightly higher values of T_{CoCo} compared to those of T_{FeFe} are found for alloys with metalloid content up to 22 at. %. The values of T_{FeFe} are all in the range of 630 ± 50 K, while big differences are found in T_{CoCo} values: T_{CoCo} corresponding to the present alloys series, representing the Curie temperature of $\text{Co}_{70}(\text{C,B,Si,Al,Ga,P})_{30}$, is around 400 K lower than that of a Co based alloy with a 25 at. % metalloid content and 200 K higher than that of $\text{Co}_{62.5}\text{Si}_{12.5}\text{B}_{25}$ amorphous alloy.⁴ These results indicate that the influence of metalloid content on the exchange interaction of Co–Co atoms pairs is much larger than on Fe–Fe atoms pairs, as previously suggested.⁴ This fact can be explained as due to an increase of the average distance between Fe–Fe and Co–Co atoms pairs with increasing metalloid content. As it has been stated by theoretical calculations, in the case of pure amorphous Co, the exchange coupling tends to strengthen when the Co–Co interatomic distance decreases, while in the case of the pure amorphous Fe, a dependence of the exchange interaction with the interatomic distance is not observed.¹⁰

B. Mössbauer spectrometry

Mössbauer spectra of as-quenched samples taken at 77 K (Fig. 3) and at 300 K (Fig. 4) show the broad and asymmetric six-line pattern characteristic of amorphous ferromagnetic alloys. The data were fitted using a discrete hyperfine mag-

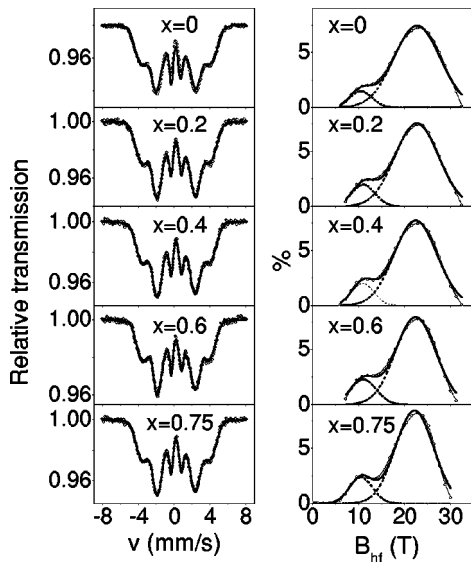


FIG. 3. Transmission Mössbauer spectra at 77 K and their corresponding fitting (solid line) and hyperfine magnetic field distributions (right) of $Fe_3Co_2B_xC_wSi_3Al_5Ga_2P_{10}$ (Table I) amorphous alloys as a function of the relative Co/(Fe+Co) content, x .

netic field distribution (HFD) with the quadrupolar splitting averaged to zero. In order to reproduce the asymmetrical shape of the spectra, a linear correlation between the hyperfine magnetic field and the isomer shift of the components of the distribution was introduced.¹¹

Figure 5(a) shows the average hyperfine magnetic field, $\langle B_{hf} \rangle$, at 77 and 300 K, as a function of x . The decrease of $\langle B_{hf} \rangle$ with the Co content of the alloy is in accordance with the observed dependence of the average magnetic moment per transition metal atom (TM),² $\langle \mu_{TM} \rangle$, that is also given in Fig. 5(b).

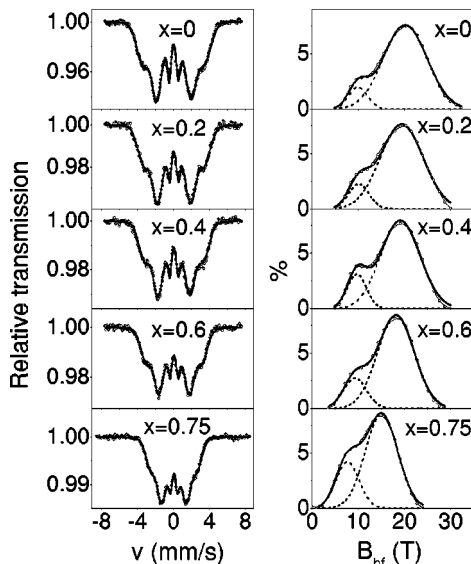


FIG. 4. Transmission Mössbauer spectra at 300 K and their corresponding fitting (solid line) and hyperfine magnetic field distributions (right) of $Fe_3Co_2B_xC_wSi_3Al_5Ga_2P_{10}$ (Table I) amorphous alloys as a function of the relative Co/(Fe+Co) content, x .

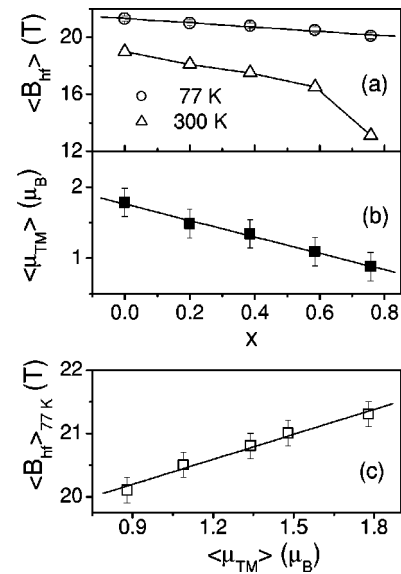


FIG. 5. Average hyperfine magnetic field, $\langle B_{hf} \rangle$, at 77 and 300 K (a) and average magnetic moment per transition metal, $\langle \mu_{TM} \rangle$, (b) of $Fe_3Co_2B_xC_wSi_3Al_5Ga_2P_{10}$ (Table I) amorphous alloys as a function of their relative Co/(Fe+Co) content, x . Average hyperfine magnetic field, $\langle B_{hf} \rangle$, at 77 K (c) as a function of $\langle \mu_{TM} \rangle$.

The decrease of $\langle \mu_{TM} \rangle$ as the Co content of the alloy increases can be explained by the simple substitution of Fe by Co moments, assuming both magnitudes to be constant over the concentration range studied, as can be inferred from the experimental linear relationship

$$\langle \mu_{TM} \rangle = \mu_{Fe}(1-x) + \mu_{Co}x, \quad (2)$$

where $\mu_{Fe} = 1.76(8) \mu_B$ is the average Fe moment of the Co free alloy and $\mu_{Co} = 0.60(8) \mu_B$ is the average Co moment of the Fe free alloy. The lower values of the magnetic moments of both Fe and Co in the amorphous alloys compared to those of pure Fe and Co, respectively, can be explained as due to $p-d$ hybridization, which has to be stronger in the case of Co as compared to Fe and thus the expected relative decrease in the magnetic moment has to be larger for Co than for Fe, in agreement with the experimental data.¹²

It is well known that the main contribution to the Fe hyperfine magnetic field in amorphous alloys arises from the Fermi contact term, which is proportional to the spin density at the Fe nucleus.^{13,14} This quantity can be decomposed into a core contribution and a valence contribution. The Fe core contribution is considered to be proportional to the average magnetic moment of the Fe atom in the alloy (or to its d component which is nearly the same) while the valence contribution, which roughly scales with the s component of this magnetic moment, accounts for the contribution of the rest of the alloy and can be considered to be proportional to the surrounding moments $\langle \mu_{TM} \rangle$:¹²

$$\langle B_{hf} \rangle = a\langle \mu_{Fe} \rangle + b\langle \mu_{TM} \rangle. \quad (3)$$

In the case of the $FeCoSiAlGaPCB$ amorphous alloys studied, the linear dependence of the low temperature $\langle B_{hf} \rangle$ on $\langle \mu_{TM} \rangle$, shown in Fig. 5(c), can be expressed using the relationship

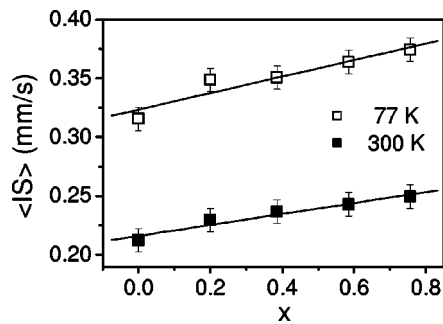


FIG. 6. Average isomer shift, $\langle IS \rangle$, at 77 and 300 K, of $\text{Fe}_{70}\text{Co}_2\text{B}_u\text{C}_w\text{Si}_3\text{Al}_5\text{Ga}_2\text{P}_{10}$ (Table I) amorphous alloys, as a function of their relative Co/(Fe+Co) content, x .

$$\langle B_{\text{hf}} \rangle (T) = 19.0(3) + 1.3(3) \langle \mu_{\text{TM}} \rangle (\mu_B). \quad (4)$$

Such linear dependence has been previously observed in Fe–Co and Fe–Ni based amorphous alloys.^{12,15,16} Assuming a constant average Fe magnetic moment of the alloy over the whole range of linearity and taking for it the value of $1.76 \mu_B$ (for $\text{Fe}_{70}\text{Si}_3\text{Al}_5\text{Ga}_2\text{P}_{10}\text{C}_5\text{B}_5$), coefficients a and b of Eq. (3) take the values $10.8(8) \text{ T}/\mu_B$ and $1.3(3) \text{ T}/\mu_B$, respectively.

The value of the coefficient a is slightly lower than those found, around $12.5 \text{ T}/\mu_B$, on a number of amorphous alloys.¹³ The small value of coefficient b shows that substitution of Fe by Co does not influence strongly the value of $\langle B_{\text{hf}} \rangle$ supporting the constancy of $\langle \mu_{\text{Fe}} \rangle$ and consequently that of $\langle \mu_{\text{Co}} \rangle$ through Eq. (2). The small contribution of the second term in Eq. (3) can be explained as due to the small electronic free path in amorphous alloys due to structural disorder.^{13,14}

The concentration dependence of the average hyperfine magnetic field is modified with increasing temperature [Fig. 5(a)]. The steeper decrease of $\langle B_{\text{hf}} \rangle$ with x at 300 K compared to that at 77 K can be attributed to the decrease in the Curie temperature of the alloy with increasing Co content in the composition range studied.

Figure 6 shows the dependence of average isomer shift, $\langle IS \rangle$, at 77 and 300 K as a function of x . A linear increase of $\langle IS \rangle$ with x was also found in $(\text{FeCo})_{80}\text{B}_{20}$ ¹² and $(\text{FeCo})_{77}\text{B}_{13}\text{Si}_{10}$ ¹⁷ amorphous alloys. Values of IS are closely related to the s electronic charge densities at the nuclei. The interpretation of IS at Fe nuclei is usually based on the idea that the total density of electronic charge at the nucleus is the sum of a valence contribution from $4s$ -like electrons which depends mainly on the number of $4s$ electrons at the Fe atom and a core contribution due to the $3s$ electrons which reflects, through the shielding effect, the number of $3d$ -like electrons at the Fe atom. The monotonous increase of the isomer shift with Co concentration could be explained as due to an increase in the $3d$ electron density or a decrease in the $4s$ electron density or both at the Fe sites.^{18,19} Preferential electron transfer from B to Fe with increasing Co concentration, due to the higher density of states in the Fe d band and therefore a stronger screening effect of the conduction electrons at the Fe sites, could be an explanation.¹²

The standard deviation of the hyperfine field distribution, $\sigma_{\text{HFD}} = [\langle B_{\text{hf}}^2 \rangle - \langle B_{\text{hf}} \rangle^2]^{1/2}$, versus x , for spectra at 77 and 300

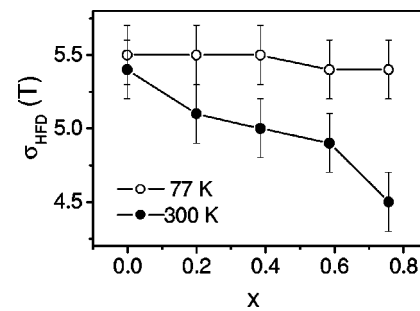


FIG. 7. Standard deviation of the distribution of hyperfine magnetic fields, σ_{HFD} , at 77 and 300 K, of $\text{Fe}_{70}\text{Co}_2\text{B}_u\text{C}_w\text{Si}_3\text{Al}_5\text{Ga}_2\text{P}_{10}$ (Table I) amorphous alloys, as a function of their relative Co/(Fe+Co) content, x .

K, is shown in Fig. 7. Its value at 77 K does not show any change with Co substitution within the experimental error ($\pm 0.1 \text{ T}$). Thus, it can be concluded that short range order around the Fe atoms, defined by the distances between the Fe atom and its nearest neighbors and the probability of distribution of the different atoms around the Fe one, does not significantly change with Co substitution. On the contrary, σ_{HFD} at room temperature decreases with increasing Co content. Therefore, the narrowing of the HFD at 300 K with increasing Co content can be considered as an artifact caused by the different Curie temperatures of the samples that makes the measurements at room temperature not directly comparable.

The hyperfine magnetic field distributions corresponding to Mössbauer spectra of the studied alloys at 77 and 300 K, are shown in Figs. 3 and 4 (right-hand side), respectively. Their bimodal behavior reveals the presence of two main kinds of iron environments in the amorphous as-cast state. HFDs can be approximately described by means of two “gaussian” components. The high field (HF) component can be ascribed to sites where Fe atoms are preferentially surrounded by Fe, Co, Si (Al,Ga,P) and B (C) atoms and the low field (LF) one to Fe atoms preferentially surrounded by B (C) atoms.²⁰

In order to make easier the discussion of the changes in the HFDs with x , peak position, width, and intensity of the two gaussian components, HF and LF, are plotted in Fig. 8. It should be noted for spectra at 77 K: (i) the independence of the peak position of the LF component on Co content and the small shift of the HF peak to lower values as the Co content of the alloy increases. Both results are in accordance with our previous assignment of atomic environments of Fe atoms for both components. (ii) The slight decrease of the width of the HF gaussian with x , suggesting a small increase in the short range order around the Fe atoms preferentially surrounded by Fe, Co, Si (Al,Ga,P) and B(C) with increasing Co content. The existence of chemical preferences leading the B atoms to locate near Fe atoms and Si near Co, found previously in $(\text{FeCo})_{75}\text{Si}_{15}\text{B}_{10}$ metallic glasses,²¹ can be the origin of the small increase of the short range order in the Co-rich side alloys. (iii) The increase of the area of the LF peak with x corroborates this assumption. Changes in the HFD corresponding to spectra at room temperature can be explained taking into account the earlier considerations for

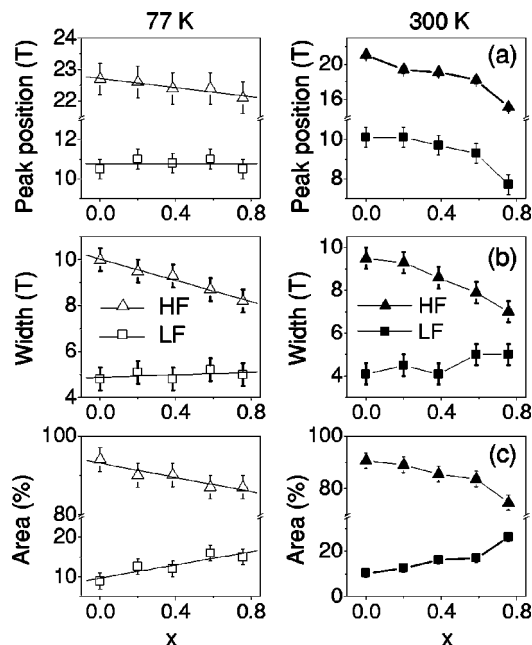


FIG. 8. Peak position (a), width (b) and area (c) of the two gaussian components resulting of the fitting of the hyperfine magnetic field distributions of Figs. 3 and 4 for $Fe_yCo_zB_uC_wSi_3Al_5Ga_2P_{10}$ (Table I) amorphous alloys, as a function of their relative Co/(Fe+Co) content, x .

HFD at 77 K and the difference of the Curie temperature of the alloys.

The relative intensities of the lines of the spectra contain information on the orientation of the internal magnetic field in the absorber. In particular, there is a direct dependence between the angle θ , defined by the direction of the hyperfine magnetic field and the propagation direction of the γ rays, and the intensities of the second and the third absorption lines of the spectra given by the relation $I_{2,3} = (4 \sin^2 \theta) / (1 + \cos^2 \theta)$. The values of θ at 300 K, shown in Fig. 9(a), indicate the presence of an in-plane texture of magnetic moments for all alloys, which decreases linearly with the Co

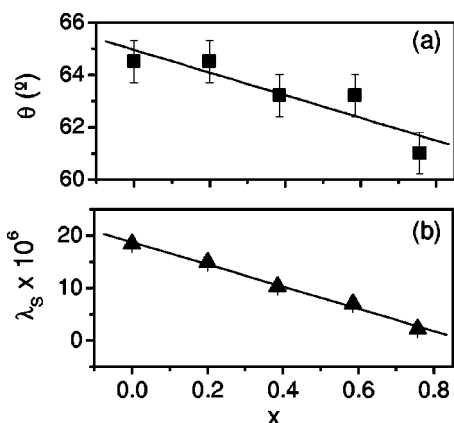


FIG. 9. Angle θ defined by the direction of the hyperfine magnetic field and the propagation direction of the γ rays (a), and saturation magnetostriction, λ_s , (b),² of $Fe_yCo_zB_uC_wSi_3Al_5Ga_2P_{10}$ (Table I) amorphous alloys, as a function of their relative Co/(Fe+Co) content, x .

content of the alloy as does the saturation magnetostriction, λ_s ,² [Fig. 9(b)]. This preferential orientation is consistent with the presence of large quenched-in stresses.

IV. CONCLUSIONS

A Mössbauer spectrometry, at 77 and 300 K, and a magnetic study of amorphous $(FeCoBC)_{80}Si_3Al_5Ga_2P_{10}$ alloys provides strong evidence for the presence of Fe and Co constant magnetic moments with values around those of Co-free alloy and Fe-free alloy, respectively, for the compositional range studied. The most important argument in this respect is the linear dependence of the low temperature average hyperfine magnetic field on the average magnetic moment per transition metal atom and the small change of $\langle B_{hf} \rangle$ of only 6% over a compositional range in which the $\langle \mu_{TM} \rangle$ changes by approximately 65%. The presence of two main types of iron environments in the amorphous as-cast alloys can be concluded, corresponding to Fe atoms preferentially surrounded by Fe, Co, Si (Al,Ga,P), and B(C) atoms and Fe atoms preferentially surrounded by B(C) atoms. The existence of chemical preferences leading the B atoms to locate near Fe atoms and Si atoms near Co atoms can be the origin of the small increase of the short range order in the Co-rich side alloys. All alloys show the presence of an in-plane texture of magnetic moments, that decreases with the Co content of the alloy as does the saturation magnetostriction.

ACKNOWLEDGMENTS

This work was partially supported by Spanish Ministry of Science and Technology and EU-FEDER (Project No. MAT2001-3175), the PAI of the Junta de Andalucía, and the Acción Integrada Hispano-Alemana HA2002-0077.

- ¹A. Inoue, A. Makino, and T. Mizushima, *J. Magn. Magn. Mater.* **215–216**, 246 (2000).
- ²J. M. Borrego, A. Conde, S. Roth, and J. Eckert, *J. Appl. Phys.* **92**, 2073 (2002).
- ³R. A. Brand, J. Lauer, and D. M. Herlach, *J. Phys. F: Met. Phys.* **12**, 675 (1983).
- ⁴B. G. Shen, L. Cao, and H. Q. Guo, *J. Appl. Phys.* **73**, 5730 (1993).
- ⁵F. E. Luborsky, *J. Appl. Phys.* **51**, 2808 (1980).
- ⁶M. L. Fernández-Gubieda, I. Orue, J. M. Barandiaran, and F. Plazaola, in *Non-Crystalline and Nanoscale Materials*, edited by R. Rivas and M. A. López Quintela (World Scientific, Singapore, 1997), p. 172.
- ⁷J. S. Kouvel, in *Magnetism and Metallurgy*, edited by A. E. Berkowitz and E. Kneller (Academic, New York, 1969), p. 523.
- ⁸C. F. Conde and A. Conde, *Mater. Sci. Forum* **269–272**, 719 (1998).
- ⁹M. Knobel, R. Sato Turtelli, and R. Grössinger, *J. Magn. Magn. Mater.* **116**, 154 (1992).
- ¹⁰R. F. Sabiryanov, S. K. Bose, and O. N. Mryasov, *Phys. Rev. B* **51**, 8958 (1995).
- ¹¹I. Vincze, *Solid State Commun.* **25**, 689 (1978).
- ¹²S. Dey, P. Deppe, M. Rodenberg, F. E. Luborsky, and J. L. Walter, *J. Appl. Phys.* **52**, 1805 (1981).
- ¹³P. Panissod, J. Durand, and J. I. Budnick, *Nucl. Instrum. Methods Phys. Res.* **199**, 99 (1982).
- ¹⁴T. Kemeny, B. Fogorassy, I. Vincze, J. W. Donald, M. J. Besnus, and H. A. Davies, in *Proceedings of the Fourth International Conference on Rapidly Quenched Metals*, edited by T. Matsumoto and K. Suzuki (Japan Institute of Metals, Sendai, 1982), Vol. 2, p. 851.
- ¹⁵C. L. Chien, D. P. Musser, F. E. Luborsky, J. J. Becker, and J. L. Walter, *Solid State Commun.* **24**, 231 (1977).
- ¹⁶H. Franke, S. Dey, M. Rosenberg, F. E. Luborsky, and J. L. Walter, *J. Magn. Magn. Mater.* **15–18**, 1346 (1980).

¹⁷M. A. Mostafá, J. Valgo, and E. Kuzmann, *Phys. Status Solidi A* **96**, 445 (1986).

¹⁸R. Ingalls, *Phys. Rev. B* **155**, 157 (1967).

¹⁹L. R. Walker, G. K. Wertheim, and V. Jaccarino, *Phys. Rev. Lett.*

6, 98 (1961).

²⁰M. Miglierini, *J. Phys.: Condens. Matter* **6**, 1431 (1994).

²¹I. Orúe, M. L. Fernández-Gubieda, F. Plazaola, and J. M. Barandiarán, *J. Phys.: Condens. Matter* **10**, 3807 (1998).